

# A simple method to simulate $W/Z + \text{jet}$ production at hadron collisions with PS-ME matching

---

**Shigeru Odaka**

*High Energy Accelerator Research Organization (KEK)  
1-1 Oho, Tsukuba, Ibaraki 305-0801, Japan  
E-mail: shigeru.odaka@kek.jp*

ABSTRACT: We propose a simple method to simulate  $W/Z + \text{jet}$  productions at hadron collisions. The simulation can be done by using existing tools with some modifications allowed to users.  $W/Z + 1 \text{ jet}$  events are generated using an ME-based event generator at the tree level. The divergence at low  $p_T$  is suppressed by using the Sudakov form factor. PS is added with an appropriate consideration for PS-ME matching. The simulation for the  $W + 1 \text{ jet}$  production shows a smooth matching with the  $W + 0 \text{ jet}$  simulation at low  $p_{Ts}$ . The  $Z + 1 \text{ jet}$  simulation in the Tevatron Run I condition well reproduces the experimental measurement on the  $p_T$  spectrum of  $Z$ .

KEYWORDS: Hadronic Colliders, Jets, QCD.

---

## Contents

<b>1. Introduction</b>	<b>1</b>
<b>2. <math>W + 1</math> jet simulation</b>	<b>2</b>
<b>3. Sudakov form factor</b>	<b>4</b>
<b>4. Suppressed <math>W + 1</math> jet simulation</b>	<b>7</b>
<b>5. <math>Z</math> production at Tevatron Run I</b>	<b>9</b>
<b>6. Conclusion</b>	<b>11</b>

---

## 1. Introduction

The simulation of multiple hadron jet (multi-jet) production is one of the most serious problems in physics analyses at high-energy hadron collider experiments. Our experimental reach extends to heavier objects as the collision energy increases. Once such heavy objects decay hadronically, they frequently produce multi-jet final states. Similar multi-jet configuration originating from well-separated emission of light quarks and/or gluons can be easily produced by non-resonant QCD interactions. They may blind or distort interesting heavy object signals. We have already encountered this problem in the study of hadronic top-quark decays at Tevatron. The problem will become much more severe for heavier objects (Higgs boson(s), SUSY particles, *etc.*) expected at forthcoming LHC experiments, since in principle the signal frequency decreases as the cm energy of the hard interaction increases while the QCD activity remains nearly constant. Understanding of the QCD multi-jet production will become crucial for the study of such heavy objects. Despite that, the technique is not well established for the simulation.

The simulation of hadron collision interactions consists of two components: parton showers (PS) describing relatively soft regions in the initial-state and the final-state interactions, and a simulation of hard interactions based on perturbative matrix-element (ME) calculations. The former is a 3-dimensional model based on the factorization theory, adding the contributions of large collinear components to all orders. The matching between the two components is important, but is not trivial since theoretical discussions are usually made only at the collinear limit where transverse behaviors are ignored. A certain model-based discussion is necessary to construct a consistent multi-jet simulation.

Recently, the CKKW technique originally proposed for the final-state jet production at  $e^+e^-$  collisions [1] has been extended to the initial state [2], and implemented in an

event generator for hadron collisions [3]. This technique consistently adds tree-level ME calculations for a certain hard interaction process associated with 0 jet, 1 jet, 2 jets, ..., to provide an exclusive event sample above a certain resolution scale. A PS is applied to a limited phase space which ME calculations do not cover, with a careful consideration for the matching. The concept is also implemented in different ways in other event generators [4].

CKKW provides us with an exclusive multi-jet sample. Despite, in many cases, users are interested only in an inclusive behavior of a certain number of leading jets. They ignore non-leading ones in order to make the evaluation as free from theoretical and experimental ambiguities in soft regions as possible. We expect that there must be a simpler method for such applications. In this paper we propose a method to obtain a simulation sample of inclusive  $n$ -jet events by using an  $n$ -jet ME event generator with the help of an appropriate PS simulation.

In the present study we focus on the simplest case, the  $W + 1$  jet production. Namely, we are interested only in the leading-jet behavior produced in association with the  $W$  boson production. This process deals with the jet emission from the initial-state partons only. The discussions would be able to extend to the final state with appropriate replacements of the parameters and formulae. We use only those tools which are publicly available. Modifications are applied at the level where ordinary users are allowed. We apply our method to the  $Z + 1$  jet production in the Tevatron Run I condition for a comparison with experimental measurements. The  $Z$  production is used only because the momentum measurement is expected to be less ambiguous than the  $W$  production.

## 2. $W + 1$ jet simulation

The  $W + 1$  jet production is simulated at the tree level by using GR@PPA version 2.76 [5] together with the PS in PYTHIA version 6.212 [6] in the present study. The  $W$  bosons always decay to the pair of an electron and a neutrino. GR@PPA includes this decay in the ME calculation. The sample program in the GR@PPA distribution package is used for interfacing GR@PPA and PYTHIA. Studies are done for the LHC condition, proton-proton collisions at the cm energy of 14 TeV. A CTEQ6L1 [7] routine included in the sample program is used for PDF.

Both the initial and final state PSs are activated in PYTHIA with the default setting, while the hadronization and the multiple interaction are deactivated for simplicity ( $\text{MSTP}(81) = 0$  and  $\text{MSTP}(111) = 0$ ). The QED radiation is also deactivated ( $\text{MSTJ}(41) = 1$ ). A jet clustering (PYCELL in PYTHIA) is applied to the parton-level events, where the detector is assumed to cover the full azimuth ( $\phi$ ) and the pseudorapidity ( $\eta$ ) up to 4.5 in the absolute value with a granularity of about 0.1 in both  $\phi$  and  $\eta$ . The jets are reconstructed using a cone algorithm with the half-cone size of 0.4 in  $R$  and with the transverse energy ( $E_T$ ) threshold of 10 GeV.

A naive simulation of this process has an obvious difficulty. In hadron collision simulations we have to give four energy scales: renormalization scale ( $\mu_R$ ), factorization scale ( $\mu_F$ ), and energy scales for the initial-state PS ( $\mu_{\text{ISR}}$ ) and the final-state PS ( $\mu_{\text{FSR}}$ ). It is

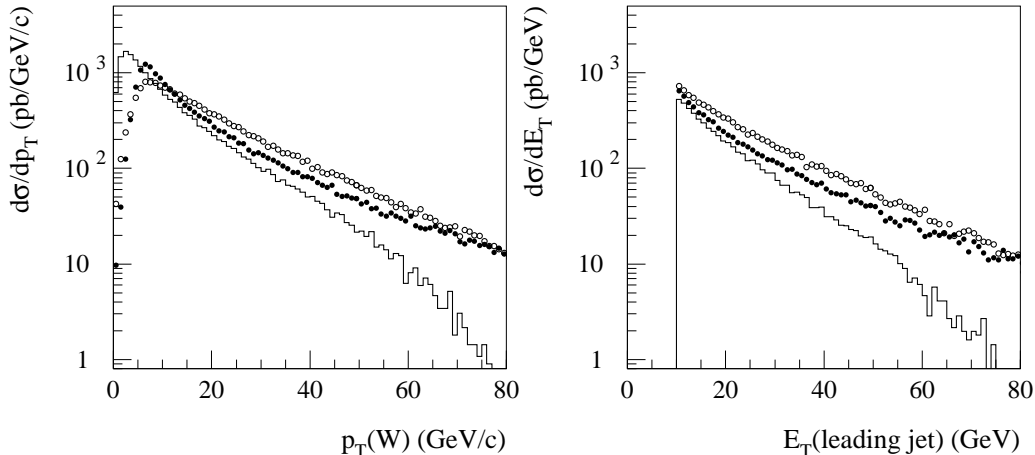


**Figure 1:** Naive simulation of  $W + 1$  jet production at LHC. The  $p_T$  distribution of the  $W$  boson and the  $E_T$  distribution of the leading jet are plotted. The  $W + 1$  jet events are generated by GR@PPA 2.76 with the  $\hat{p}_T$  cut of 5 GeV/ $c$ , and the PYTHIA PS is applied to the initial and final states with the default setting. A  $E_T$  cut of 10 GeV is imposed in the jet reconstruction. Results for two extreme cases of the energy-scale choice are shown:  $\mu = \hat{p}_T$  with solid circles, and  $\mu = m_W$  with open circles. Histograms show the results from the  $W + 0$  jet simulation with  $\mu = m_W$ .

usually said that they should be set to the *typical* energy scale of the interaction. However, there are two energy scales in the  $W + 1$  jet production: the  $W$ -boson mass ( $m_W$ ) and the transverse momentum ( $p_T$ ) of the jet. They can be quite different from each other if we allow very low  $p_T$  ( $\sim 10$  GeV/ $c$ ) for the jet.

Figure 1 shows the simulation results for the  $p_T$  distribution of  $W$  and the  $E_T$  distribution of the leading jet (the highest  $E_T$  jet). The ME events are generated with a minimum  $p_T$  cut of 5 GeV/ $c$  in the cm frame of the hard interaction. Distributions are shown for two extreme cases of the energy-scale choice. All energy scales are defined to be identical and set equal to the jet  $p_T$  in the cm frame ( $\hat{p}_T$ ) in one case, and the  $W$  mass (the invariant mass of the electron and neutrino) in the other. These choices are non-standard in GR@PPA. The user-define option (ICOU = IFACT = 6) is selected, and the energy-scale parameters (GRCQ and GRCFAQ) are appropriately set in the subroutine GRCUSRSETQ. We frequently see similar simulations in previous  $W +$  jets analyses. The figure shows that the difference is significant not only in the absolute value but also in the shape.

The prediction from the  $W + 0$  jet event generator in GR@PPA 2.76 is also shown in Fig. 1. The same PYTHIA PS is applied with all the energy scales set equal to the  $W$  mass. The finite  $p_T$  of  $W$  and all jet activities are generated by PS in this case. The low  $p_T$  behavior must be well described by this simulation. However, neither the two  $W + 1$  jet simulations agrees with it at low  $p_T$ s. The  $\mu = \hat{p}_T$  simulation looks better around  $p_T = 20$  GeV/ $c$ , but deviates at further low  $p_T$ s. This is unavoidable since the  $W + 1$  jet cross

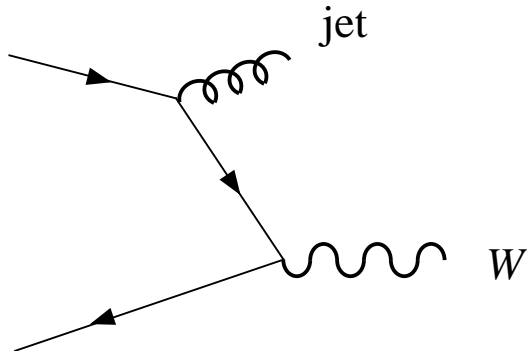


**Figure 2:** One of the Feynman diagrams for which the  $W + 1$  jet ME is evaluated.

section diverges at  $\hat{p}_T = 0$ .

Figure 2 illustrates one of the Feynman diagrams for which the  $W + 1$  jet ME is evaluated. In the present *inclusive* analysis, the jet in the ME should be identical to the leading jet that we observe. This means that there should not be any jet having  $p_T$  larger than that. The naive simulation with  $\mu = m_W$  is apparently inadequate from this point of view. The initial-state PS frequently generates high  $p_T$  jets, resulting in large cross sections in medium  $p_T$  and  $E_T$  regions in Fig. 1.

The excessive PS activities can be eliminated by the choice of  $\mu = \hat{p}_T$ . This leads to a better behavior in low  $p_T$  and  $E_T$  regions. The divergence at further low  $p_T$ s appears only because we stop the perturbation at a limited order, the lowest order in this case. Higher order corrections would produce higher  $p_T$  jets and suppress the contribution of the  $W + 1$  jet ME at low  $p_T$ s. This is considered to be the mechanism to make the actual observation finite. The suppression can be evaluated to all orders of the coupling constant in a collinear approximation in terms of the Sudakov form factor. This is the way usually adopted in QCD calculations having multiple energy scales, and the way used in PS. Therefore, the application of such a suppression with an appropriately evaluated Sudakov form factor should modify the  $W + 1$  jet simulation to match the  $W + 0$  jet simulation at low  $p_T$ s, and to be finite even at  $p_T = 0$ . We look for a suitable expression of the Sudakov form factor in the next section.

Although the choice of  $\mu = \hat{p}_T$  looks better, it is too naive to construct a realistic simulation. We reconsider the choice of energy scales and discuss about the matching between PS and ME in later sections.

### 3. Sudakov form factor

The Sudakov form factor for quarks can be described as

$$S_q(Q_1^2, Q_2^2) = \exp \left[ - \int_{Q_1^2}^{Q_2^2} \frac{dQ^2}{Q^2} \int_0^{1-\epsilon} dz \frac{\alpha_s}{2\pi} P_{q \rightarrow q}(z) \right], \quad (3.1)$$

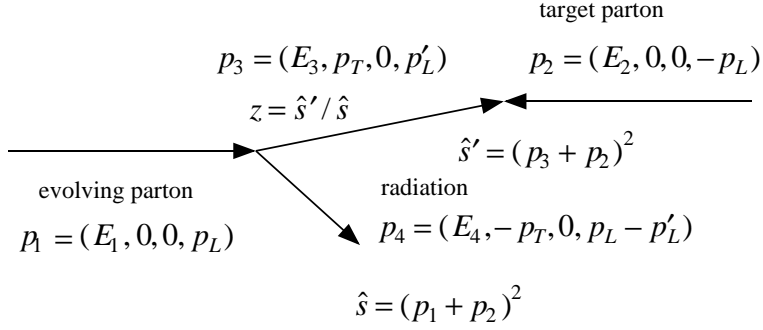


**Figure 3:** The definition of the PS splitting kinematics that we adopt.

where the splitting function for quarks with the radiation of a timelike gluon is

$$P_{q \rightarrow q}(z) = C_F \frac{1+z^2}{1-z} \quad (3.2)$$

at the leading order, with  $C_F = 4/3$ . Equation (3.1) represents the probability that a quark or an anti-quark survives without any radiation from an evolution parameter value of  $Q_1^2$  up to  $Q_2^2$ . However, the quantity is unphysical since the result depends on an artificial cutoff  $\epsilon$ . A smaller  $\epsilon$  gives a smaller  $S_q$ . This corresponds to a natural explanation that the non-radiation probability becomes smaller if we allow softer radiation, but the softness is not well defined. It is necessary to introduce a definition of the splitting kinematics in order to derive a physically meaningful quantity.

Here we examine the definition in PYTHIA for the initial-state PS [8], where  $Q^2$  is exactly the virtual of evolving partons. Details of the definition are shown in Fig. 3. The four-momenta are so defined that  $p_1^2, p_2^2$  and  $p_3^2 < 0$ , and  $p_4^2 \geq 0$ . The splitting parameter  $z$  is the ratio of the squared invariant mass of the collision system after and before the splitting, given as

$$z = \frac{\hat{s}'}{\hat{s}} = \frac{(p_3 + p_2)^2}{(p_1 + p_2)^2}. \quad (3.3)$$

This definition preserves the relation  $\hat{s}_{\text{hard}} = x_1 x_2 s$  with  $x$  given by the product of all  $z$  values in each beam. The squared four-momenta,  $\hat{s}$  and  $z$  are the inputs. The other parameters can be derived from them.

In this definition, the transverse momentum of the splitting can be described as [8]

$$p_T^2 = E_3^2 - p_L'^2 - p_3^2, \quad (3.4)$$

where

$$E_3 = \frac{\hat{s}' + p_1^2 - p_2^2 - p_4^2}{2\sqrt{\hat{s}}}, \quad p_L' = \frac{\hat{s}' - p_2^2 - p_3^2 - 2E_2 E_3}{2p_L},$$

with

$$p_L^2 = \frac{(\hat{s} - p_1^2 - p_2^2)^2 - 4p_1^2 p_2^2}{4\hat{s}}, \quad E_2 = \frac{\hat{s} - p_1^2 + p_2^2}{2\sqrt{\hat{s}}}.$$

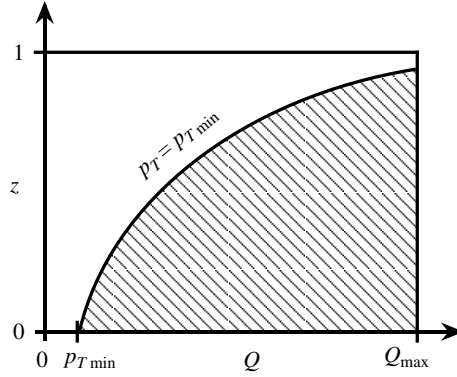


**Figure 4:** The integration area defined by the  $\theta$  function in Eq. (3.7).

In order to simplify the relation we assume the radiation to be massless ( $p_4^2 = 0$ ), and take the limit  $p_2^2 \rightarrow 0$  since fundamental properties should not depend on not-well-defined target virtuality. Furthermore, we take the limit  $p_3^2 \rightarrow p_1^2 = -Q^2$  since Eq. (3.1) indicates that we can take the virtuality step as small as we want. These approximations lead us to a relation,

$$p_T^2 = \frac{(1-z)^2 Q^2}{1 + \frac{Q^2}{\hat{s}}}. \quad (3.5)$$

If we assume  $Q^2 \ll \hat{s}$ , this can be further simplified to

$$p_T = (1-z)Q. \quad (3.6)$$

This is different from the usually quoted relation  $p_T^2 = (1-z)Q^2$ , but similar to the one obtained for the HERWIG PS [9].

If we assume the relation (3.6), the Sudakov form factor giving the no-radiation probability above a certain  $p_T$  cut ( $p_{T\min}$ ) can be calculated as

$$S_q(p_{T\min}, Q_{\max}) = \exp \left[ - \int_0^{Q_{\max}^2} \frac{dQ^2}{Q^2} \int_0^1 dz \frac{\alpha_s}{2\pi} P_{q \rightarrow q}(z) \theta(p_T - p_{T\min}) \right]. \quad (3.7)$$

The integration area defined by the  $\theta$  function is schematically illustrated in Fig. 4. The  $\theta$  function naturally gives an upper bound of the  $z$  integration and an lower bound of the  $Q^2$  integration. Therefore, there is no need to introduce any artificial cutoff. Namely, the result is well-defined and must have a physical meaning. The upper bound  $Q_{\max}$  should be given by the hardest energy scale in the considered interaction. It would be natural to take the  $W$ -boson mass for non-hard radiation in the  $W + 1$  jet production. Although Eq. (3.7) is numerically calculable, it is rather complicated for the application to actual simulations.

Let's start from the radiation function which the Sudakov form factor is based on. The radiation probability is usually expressed as

$$d\Gamma = \frac{dQ^2}{Q^2} dz \frac{\alpha_s}{2\pi} P(z). \quad (3.8)$$

If we assume the relation (3.6), we obtain another expression that

$$d\Gamma = \frac{dp_T}{p_T} dz \frac{\alpha_s}{\pi} P(z). \quad (3.9)$$

Using this expression, the Sudakov form factor having the same meaning as Eq. (3.7) can be written as

$$S_q(p_{T\min}, Q_{\max}) = \exp \left[ - \int_{p_{T\min}}^{Q_{\max}} \frac{dp_T}{p_T} \int_0^{1-\frac{p_T}{Q_{\max}}} dz \frac{\alpha_s}{\pi} P_{q \rightarrow q}(z) \right]. \quad (3.10)$$

The upper bound of the  $z$  integration is given by the relation  $p_T = (1-z)Q \leq (1-z)Q_{\max}$ .

Since it is natural to define  $\alpha_s$  to be a function of  $p_T$  of the splitting, the  $z$  integration is easy to perform. Assuming the leading order function (3.2), we obtain

$$S_q(p_{T\min}, Q_{\max}) = \exp \left[ - \int_{p_{T\min}}^{Q_{\max}} \frac{2C_F}{\pi} \frac{\alpha_s(p_T)}{p_T} \left( \ln \frac{1}{\epsilon} - \frac{3-4\epsilon+\epsilon^2}{4} \right) dp_T \right] \quad (3.11)$$

with  $\epsilon = p_T/Q_{\max}$ . This leads to the expression used in the CKKW method [1] if we take the limit  $\epsilon \rightarrow 0$  in the non-divergent term, although the definition of the parameters is slightly different. The difference between Eq. (3.7) and Eq. (3.11) is only in the definition of the integration variables. They give exactly identical answers.

#### 4. Suppressed $W + 1$ jet simulation

For the test of the suppression,  $W + 1$  jet events are generated using GR@PPA 2.76 with the energy scale choice of  $\mu_R = \mu_F = \hat{p}_T$ , where  $\hat{p}_T$  is the transverse momentum of the jet and  $W$  in the cm frame of the hard interaction. The choice  $\mu_R = \hat{p}_T$  merely means that the coupling at the parton splitting is evaluated at this energy scale. A CKKW-like correction has to be applied when we have multiple QCD vertices. The other conditions are the same as those in the simulations leading to Fig. 1.

The weight factor for the suppression is defined as

$$w = S_q(\hat{p}_T, Q_{\max})^2 \quad (4.1)$$

with Eq. (3.11), where we use the first-order expression for the strong coupling:

$$\alpha_s(p_T) = \frac{4\pi}{\beta_0 \ln(p_T^2/\Lambda^2)} \quad (4.2)$$

with  $\beta_0 = 11 - 2n_f/3$  ( $n_f = 5$ ) and  $\Lambda = 0.0883$  GeV. This gives  $\alpha_s(m_Z) = 0.118$ . The hard interaction scale is given by

$$Q_{\max} = \hat{m}_T(W) = \sqrt{m_W^2 + \hat{p}_T^2}. \quad (4.3)$$

This naturally connects reasonable definitions at two extreme cases:  $Q_{\max} = m_W$  at small  $\hat{p}_T$ s and  $Q_{\max} = \hat{p}_T$  at large  $\hat{p}_T$ s. The Sudakov form factor is squared since the no-radiation condition must be required to two incoming quarks converted to the  $W$  boson. Events



generated according to the ordinary  $W + 1$  jet cross section are accepted in proportion to this weight in the subroutine GRCUSRCUT of GR@PPA. Though this degrades the event generation efficiency, the degradation is moderate in GR@PPA because the same routine is used in the initialization stage for optimizing the event generation.

We have to apply PS also to these  $W + 1$  jet events in order to obtain realistic events. Here, an appropriate care is necessary to accomplish a reasonable matching between the PS and ME. In principle the PYTHIA PS is equivalent to the numerical evaluation of the integral in Eq. (3.1). The Sudakov form factor is evaluated by carrying out the integration over the shaded area in Fig. 4. Thus, this area is covered by ME if  $p_{T\min} = \hat{p}_T$ ; *i.e.*, no radiation there. PS has to cover the rest of the area. We can easily see that the matching cannot be achieved by a simple choice of the PS energy scale. A certain *rejection* method is necessary to apply, as is done in CKKW, when we use an ordinary  $Q^2$ -ordered PS.

We adopt the following method in the present study: the PYTHIA PS is applied with the energy-scale choice of  $\mu_{PS} = \hat{m}_T(W)$ . This can be done by explicitly setting the variable SCALUP of the LHA common HEPEUP to this value in the subroutine UPEVNT. After the PS is added we investigate the parton information in the PYJETS common of PYTHIA. The PS is re-applied to the same event if there is any radiation from the initial-state partons with  $p_T \geq \hat{p}_T$ . This is an approximation since the examined  $p_T$  does not directly correspond to the  $p_T$  of each splitting. However, this method can be applied without any modification to PYTHIA routines and, what is more, it provides us with a reasonably good results as will be shown in the following. In any case, it is impossible to achieve a perfect matching using  $Q^2$ -ordered PSs. There is no splitting to produce spacelike gluons in the  $W + 1$  jet ME, while in PS such a splitting may produce the highest  $p_T$  jet although the probability must be very small. This *rejection* does not significantly affect the event generation speed, because the PS simulation is fast and the average number of trials is only 1.3 in the present condition.

Figure 5 shows the  $p_T(W)$  and  $E_T(\text{leading jet})$  distributions of the suppressed  $W + 1$  jet simulation. Only low to medium  $p_T$  and  $E_T$  regions are shown in the figure. The suppression is not significant in higher  $p_T$  ( $E_T$ ) regions. The results from a naive simulation ( $\mu = \hat{p}_T$ ) is overwritten with dashed histograms to show how the suppression works. We can see a smooth matching with the  $W + 0$  jet simulation (histograms) at low  $p_T$  ( $E_T$ ) around 15 GeV. This shows that our suppression method is reasonable.

Two results are plotted in the figure. The filled circles show the results of the simulation implementing the above PS-ME matching method, while the open circles show those without matching. The PS energy scale is set to  $\hat{p}_T$  in the latter in order to avoid the overlap with ME. The threshold behavior is more strongly smeared in the matched simulation.

The difference between the matched and unmatched simulations is more clearly seen in Fig. 6, where  $p_T(W)$  is plotted for jet-tagged events. The distribution below the  $E_T$  threshold (10 GeV) shows the collective effect of the applied PS. The result for the  $W + 0$  jet simulation obtained from the same analysis is overwritten in the figure. The matched simulation is in good agreement with the  $W + 0$  jet simulation below the threshold. This means that our matching method is well performed; namely, the PS added to the  $W + 1$

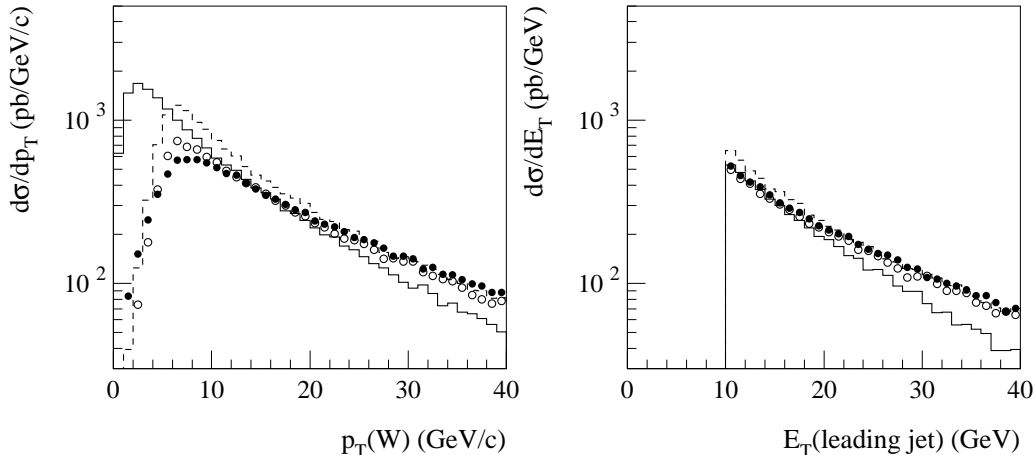


**Figure 5:** Suppressed  $W + 1$  jet simulation in the LHC condition. A  $\hat{p}_T$  cut of  $5 \text{ GeV}/c$  is applied in the hard-interaction generation, and the jet reconstruction is applied with an  $E_T$  threshold of  $10 \text{ GeV}$ . Filled circles show the results of the simulation implementing the PS-ME matching, while open circles show those without matching but with  $\mu_{PS} = \hat{p}_T$ . Dashed histograms are the naive simulation results for the energy-scale choice of  $\mu = \hat{p}_T$ . Solid histograms show the results from the  $W + 0$  jet simulation with  $\mu = m_W$ .

jet simulation is quite similar to the non-leading PS in the  $W + 0$  jet simulation. Since the leading behavior is already well matched, the suppressed  $W + 1$  jet simulation is now indistinguishable from the  $W + 0$  jet simulation at low  $p_T$ s.

Figure 7 shows the total cross section of jet-tagged events for a practical jet  $E_T$  threshold ( $20 \text{ GeV}$ ), as a function of the  $\hat{p}_T$  cut in GR@PPA. Observable quantities should not depend on artificial conditions in the simulation such as the  $\hat{p}_T$  cut. The result shows that the jet-tagged cross section is stable against the variation of the  $\hat{p}_T$  cut if it is set reasonably small. The  $\hat{p}_T$  cut of  $10 \text{ GeV}/c$  looks sufficient in the present study, though further smearing due to the hadronization and detector effects may alter it.

## 5. $Z$ production at Tevatron Run I

In this section we apply our suppressed simulation to the  $Z$  production at Tevatron for a comparison with experimental data. The simulation for the  $Z$  production ( $66 < m(Z \rightarrow e^+e^-) < 116 \text{ GeV}/c^2$ ) is compared with CDF data at Tevatron Run I [10] in Fig. 8. The result from the suppressed  $Z + 1$  jet simulation for the Tevatron Run I condition ( $\bar{p}p$  collisions at  $1.8 \text{ TeV}$  in the cm energy) is shown with the histogram. A  $\hat{p}_T$  cut of  $5 \text{ GeV}/c$  is applied again. The simulation is essentially the same as that for the  $W + 1$  jet production, except for the overall normalization. The simulation result is multiplied by a factor of  $1.48$ , the ratio between the measured inclusive  $Z$  production cross section and the

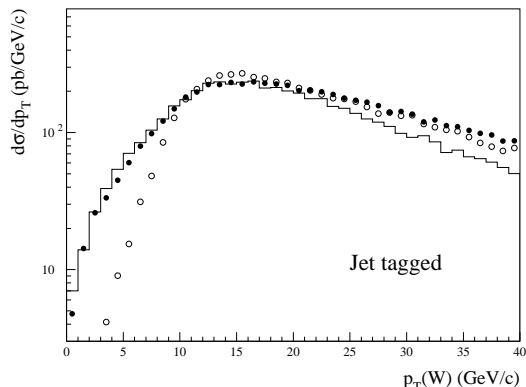


**Figure 6:** The  $p_T$  distribution of  $W$  for jet-tagged events. Filled circles show the result of the simulation to which the PS-ME matching method is applied, while open circles without the matching but with the PS energy-scale choice of  $\mu_{PS} = \hat{p}_T$ . The histogram shows the result of the same analysis applied to the  $W + 0$  jet simulation.

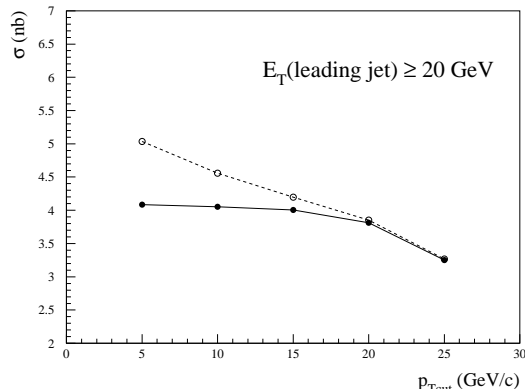


**Figure 7:** Total cross section of jet-tagged events ( $E_T \geq 20$  GeV) as a function of the  $\hat{p}_T$ -cut in the hard-interaction generation. Filled circles show the results from the suppressed  $W + 1$  jet simulation with the PS-ME matching. Open circles show those we obtain if we omit the *rejection* procedure in the matching.

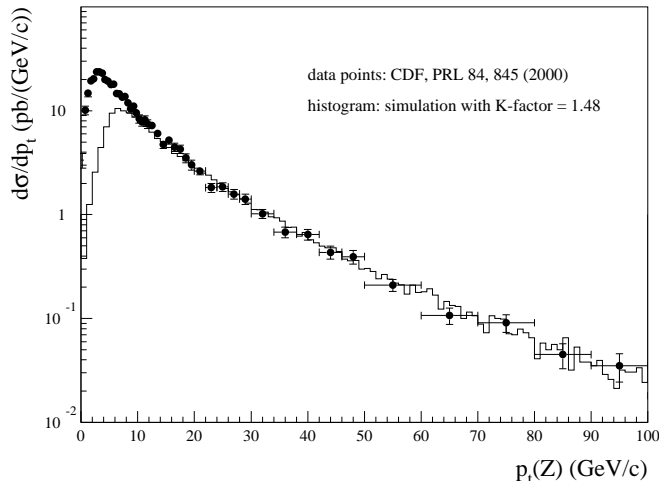


**Figure 8:** Comparison with CDF data at Tevatron Run I for the  $p_T$  spectrum of  $Z$ . The histogram shows the simulation result for the  $Z + 1$  jet production with the  $\hat{p}_T$  cut of 5 GeV/ $c$ .

corresponding tree-level prediction by the  $Z + 0$  jet generator in GR@PPA. We can see a very good agreement from low ( $\sim 15$  GeV/ $c$ ) to very high ( $\sim 100$  GeV/ $c$ )  $p_T$  regions. It should be noted that we have obtained this simulation result without any tuning.

Unfortunately jet spectrum data are not available for the comparison. There would be a difficulty in the presentation of experimental data since *jets* are experiment and analysis

dependent. By the way, there is no reason that experimental data much differ from our simulation, since the agreement is very good in the  $p_T(Z)$  spectrum. At the 0th order, the leading jet should be balanced with  $Z$  in  $p_T$ . Though higher order effects violate the balance, the dominant leading-order corrections are taken into account by applying a PS in our simulation. Thus, significant deviation can emerge only if we examine a quantity relevant to the next-to-leading jet. Note that the events generated by GR@PPA are passed to PYTHIA with the energy scale choice of  $\mu_{PS} = \hat{m}_T(Z)$ . The final-state PS is implemented up to this scale since no rejection is applied to it.

## 6. Conclusion

We have introduced a simple method for simulating *inclusive*  $W/Z + \text{jet}$  productions at hadron collisions. The divergence of the cross section at low  $p_T$  is suppressed by using the Sudakov form factor. PS is added to the events generated by an ME-based event generator at the tree level with an appropriate consideration for matching. The simulation can be done using existing tools, GR@PPA and PYTHIA. Necessary modifications can be applied at the level where ordinary users are allowed.

The results from our  $W + 1$  jet simulation show a smooth matching at low  $p_T$ s with the  $W + 0$  jet simulation, in which jet activities are totally generated by PS. The simulation of  $Z + 1$  jet production in the Tevatron Run I condition well reproduces the CDF data for  $p_T(Z)$  measurement.

The present study deals with the jet (parton) radiation from initial-state partons only. An extension to the final state is necessary to apply our method to multi-jet productions.

The method applied in the present study is similar to the *inclusive* treatment for the highest jet-multiplicity events in CKKW [3]. The success of our method suggests that the *inclusive* simulation of  $n$ -jet events in CKKW might be enough to obtain a reasonable inclusive  $n$ -jet sample, if the resolution scale can be lowered to the level of the  $\hat{p}_T$  cut in the present study. The contribution from other multiplicity events might become insignificant.

## Acknowledgments

This work has been carried out as an activity of the NLO Working Group, a collaboration between the Japanese ATLAS group and the numerical analysis group (Minami-Tateya group) at KEK. The author wants to acknowledge useful discussions with the members: J. Kodaira, J. Fujimoto, Y. Kurihara, T. Kaneko and T. Ishikawa of KEK, S. Tsuno of Okayama University, and K. Kato of Kogakuin University.

## References

- [1] S. Catani, F. Krauss, R. Kuhn and B.R. Webber, *J. High Energy Phys.* **11** (2001) 063
- [2] F. Krauss, *J. High Energy Phys.* **08** (2002) 015;  
S. Mrenna and P. Richardson, *J. High Energy Phys.* **05** (2004) 040
- [3] SHERPA: A. Schälicke and F. Krauss, *J. High Energy Phys.* **07** (2005) 018

- [4] ALPGEN: M.L. Mangano *et al.*, <http://mlm.home.cern.ch/mlm/alpgen/>;  
ARIADNE: N. Lavesson and L. Lönnblad, *J. High Energy Phys.* **07** (2005) 054
- [5] S. Tsuno *et al.*, submitted to *Comput. Phys. Commun.*; [hep-ph/0602213](http://arxiv.org/abs/hep-ph/0602213)
- [6] T. Sjöstrand *et al.*, *Comput. Phys. Commun.* **135** (2001) 238;  
T. Sjöstrand, L. Lönnblad, S. Mrenna and P. Skands, LU TP 01-21 (Apr. 2002);  
[hep-ph/0108264](http://arxiv.org/abs/hep-ph/0108264)
- [7] J. Pumplin *et al.*, *J. High Energy Phys.* **07** (2002) 012
- [8] T. Sjöstrand, *Phys. Lett.* 157B (1985) 321;  
M. Bengtsson, T. Sjöstrand and M. van Zijl, *Z. Physik C* **32** (1986) 67
- [9] G. Marchesini and B. Webber, *Nucl. Phys.* **B 310** (1988) 461
- [10] CDF Collab., T. Affolder *et al.*, *Phys. Rev. Lett.* **84** (2000) 845